Numerical Analysis of the Effect of the Electrode Distance during the Determination of the Flammability Limits of Gases

F. Ferrero*, M. Beckmann-Kluge, V. Schröder
Federal Institute for Materials Research and Testing
*Corresponding author: Unter den Eichen 87, 12205 Berlin, fabio.ferrero@bam.de

Abstract: COMSOL Multiphysics® was used as a tool for the better understanding of the evolution of flow patterns during the induced ignition of gases. A simplified model was developed for the scope, by coupling the *weakly compressible Navier Stokes* module and the *convection and conduction* module. The current paper presents the results of the performed simulations.

Keywords: spark ignition, gas flow, temperature

1. Introduction

Within the framework of the of the expansion of the German standard DIN EN 1839:2003, it has been experimentally observed that different test apparatus have strong influence on the determination of the flammability limits of gases and might even lead to dubious results (Brandes et al., 2011).

Simulations with COMSOL Multiphysics were performed, in order to analyze the gas flow patterns during the induced ignition of gases. The distance between the electrodes was considered as parameter and varied between 10 to 40 mm. In this paper the model governing equations and the results of the performed simulations are shown.

2. Model definition

2.1 Geometry and mesh

Different test apparatus can be used for the determination of the flammability limits of gases according to international standards (Brandes et al., 2011). For the simulations in this paper the setup of the tube method according to DIN EN 1839:2003 was chosen: this consists in a glass pipe with a diameter of 60 mm and a length of 300 mm. The ignition is initiated by a spark induced between two electrodes. If a flame detachment from the electrodes with propagation over a minimum distance of 100 mm is observed or the occurrence of an aureole over the whole explosion vessel is detected, the test is considered to have experienced an ignition.

Experiments with different concentrations of gas in air are repeated, as to assess the lower and upper explosion limits.

In order to reduce computing times, a 2D section of the experimental apparatus was calculated. This is a strong simplification because the flow in the depth is not considered, but was satisfactory within the scope of this study. Domains for the air and the electrodes were computed, while glass pipe was not included. In the simulations the distance between the electrodes was varied and taken as 10, 20 and 40 mm. The geometries and meshes used are shown in Figure 1 and the mesh properties are presented in Table 1.

2.2 General assumptions and equations

For the numerical model developed, the *weakly compressible Navier Stokes* module and the *convection and conduction* module were coupled in COMSOL Multiphysics®. For the sake of simplicity, the following assumptions were taken in the simulations performed:

- the spark was considered to have a temperature of 2000 K. In order to avoid divergence problems the spark temperature was increased from the system initial temperature to the assumed 2000 K in a time corresponding to $1/10^{th}$ of the total time to be computed;
- air was considered as gas. Of course, this is not representative of a real case (air cannot ignite) but, being the scope of the model a qualitative analysis of the gas flow patterns produced by the induced ignition, this assumption was justified;
- a laminar flow was selected;
- the dilatational viscosity in the momentum equation was neglected.

The governing equations of the model are shown in Table 2. The material properties have been taken from the internal COMSOL Multiphysics® library for the electrodes (steel AISI 4340) and for the gas (air). In order to help preventing divergence problems, a constant dynamic viscosity for air was taken, namely the value at ambient temperature. The boundary settings are summarized in Table 3.

The initial temperature of the system was set to 300 K and the pressure of air at 1 bara (ambient conditions).

3. Discussion

Figure 2 to Figure 4 show the computed gas flow patterns in the simulations performed. By looking at Figure 2 and Figure 3, it seems that the buoyancy of the gas under the spark might be slowed down, due to the small distance between the electrodes (10 and 20 mm, respectively). This is not the case of Figure 4 show, where the electrodes are separated by 40 mm.

In the determination of the flammability limits of dichloromethane, a strong influence of the experimental apparatus was observed (see Brandes et al., 2011). In particular the authors were not able to detect an ignition with some of test setups employed. The simulations performed for this paper showed how a small distance between the electrodes may limit the buoyancy of the gas. A limited buoyancy might in extreme cases lead to the flame extinction and might explain the experimental results achieved.

4. Conclusions

COMSOL Multiphysics® proved helpful in understanding the flow patterns during the spark induced ignition of gases. Despite of the simplicity of the model developed, interesting results were obtained, which could enlighten the effect of the experimental setup on the determination of flammability limits of gases.

5. References

1. DIN EN 1839:2003: Bestimmung der Explosionsgrenzen von Gasen und Dämpfen. Deutsche Fassung EN 1839:2003 (in German).

2. E. Brandes, J. Milde, V. Schröder, Schwer entzündbare Gase und Dämpfe – Erweiterung der europäischen Norm EN 1839 Physikalisch-Chemische Sicherheitstechnik und Explosionsschutz, PTB-Mitteilung 1/2011 (in German).

6. Nomenclature

Symbol	Description	Unit
$c_{P,air}$	Specific heat of air	J/(kg·K)
$c_{P,steel}$	Specific heat of steel	J/(kg·K)
$\vec{F}$	Buoyancy force	N/m^3
F_z	Buoyancy force (vertical component)	N/m^3
g	Gravity acceleration	m/s^2
p	Pressure	Pa
R_s	Specific gas constant of air	J/(kg·K)
T	Temperature	K
t	Time	s
$\vec{u}$	Velocity field vector	m/s
z	Vertical dimension	m
λ_{air}	Heat conduction coefficient of air	W/(m·K)
λ_{steel}	Heat conduction coefficient of steel	W/(m·K)
η_{air}	Dynamic viscosity of air	Pa·s
ρ_{air}	Density of air	kg/m^3
$\rho_{air,ref}$	Density of air (reference)	kg/m^3
ρ_{steel}	Density of steel	kg/m^3

Figures

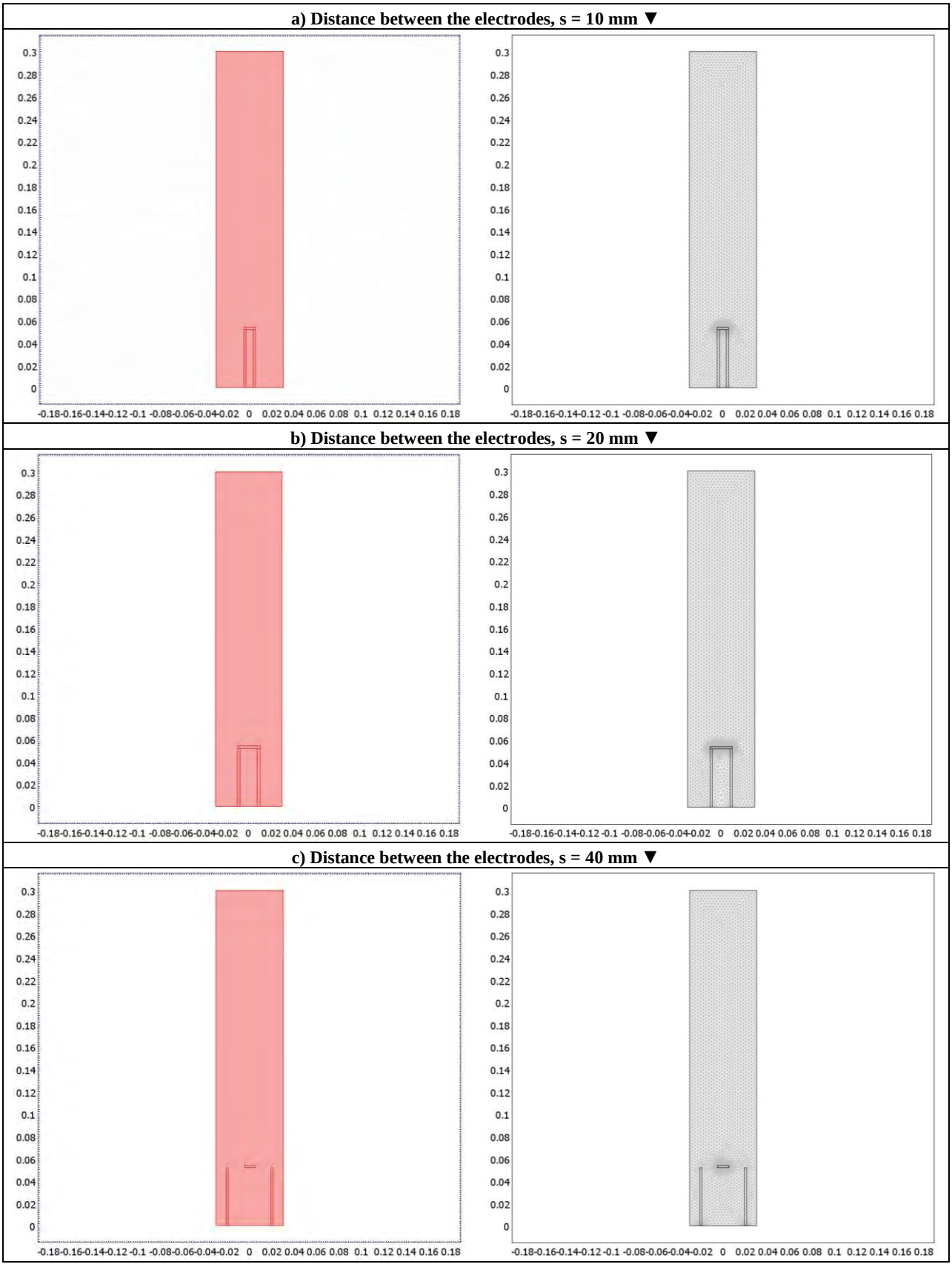

Figure 1. Geometry and meshes used in the simulations.

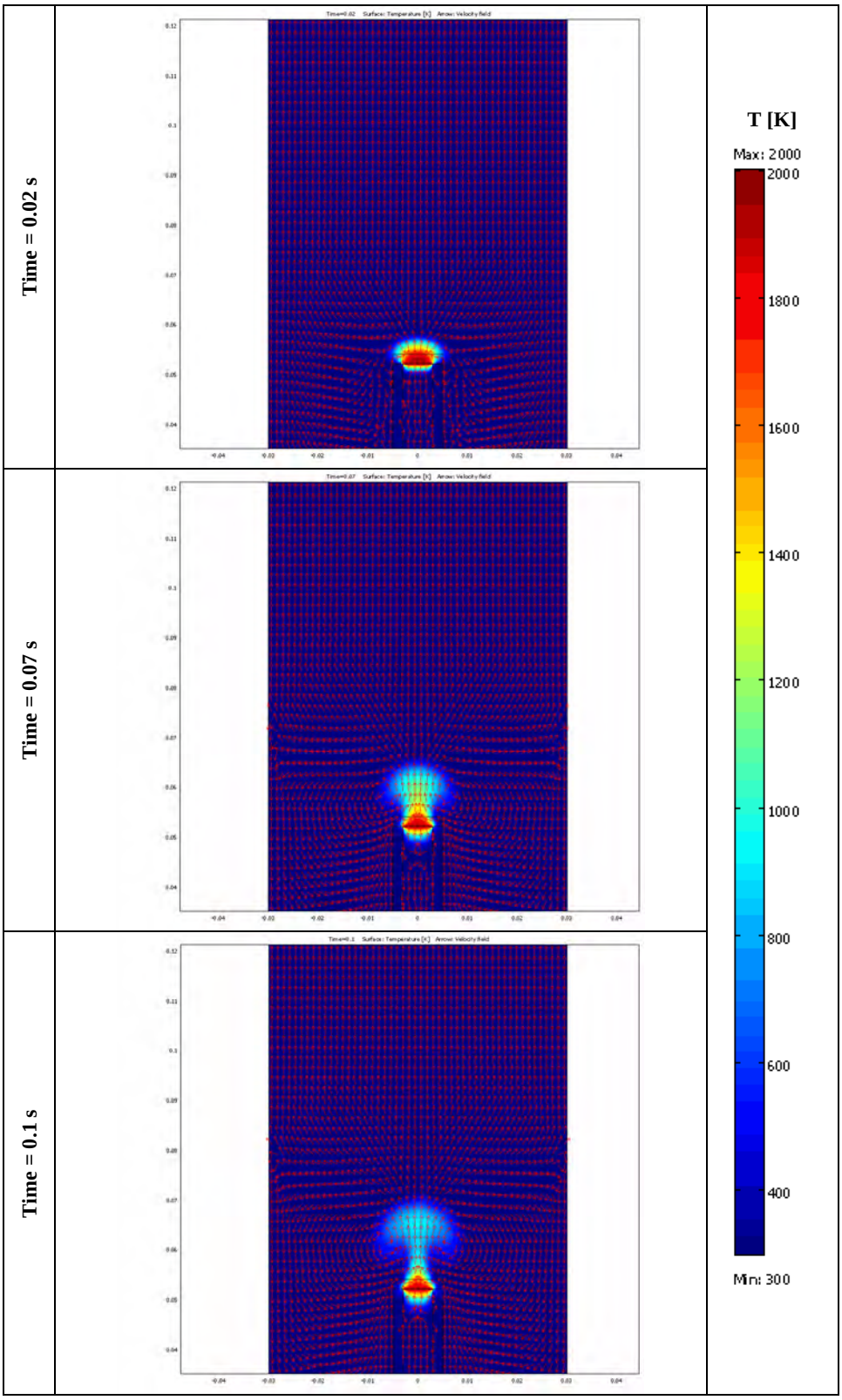

Figure 2. Temperature profile and gas flow along time, considering a distance between the electrodes of 10 mm.

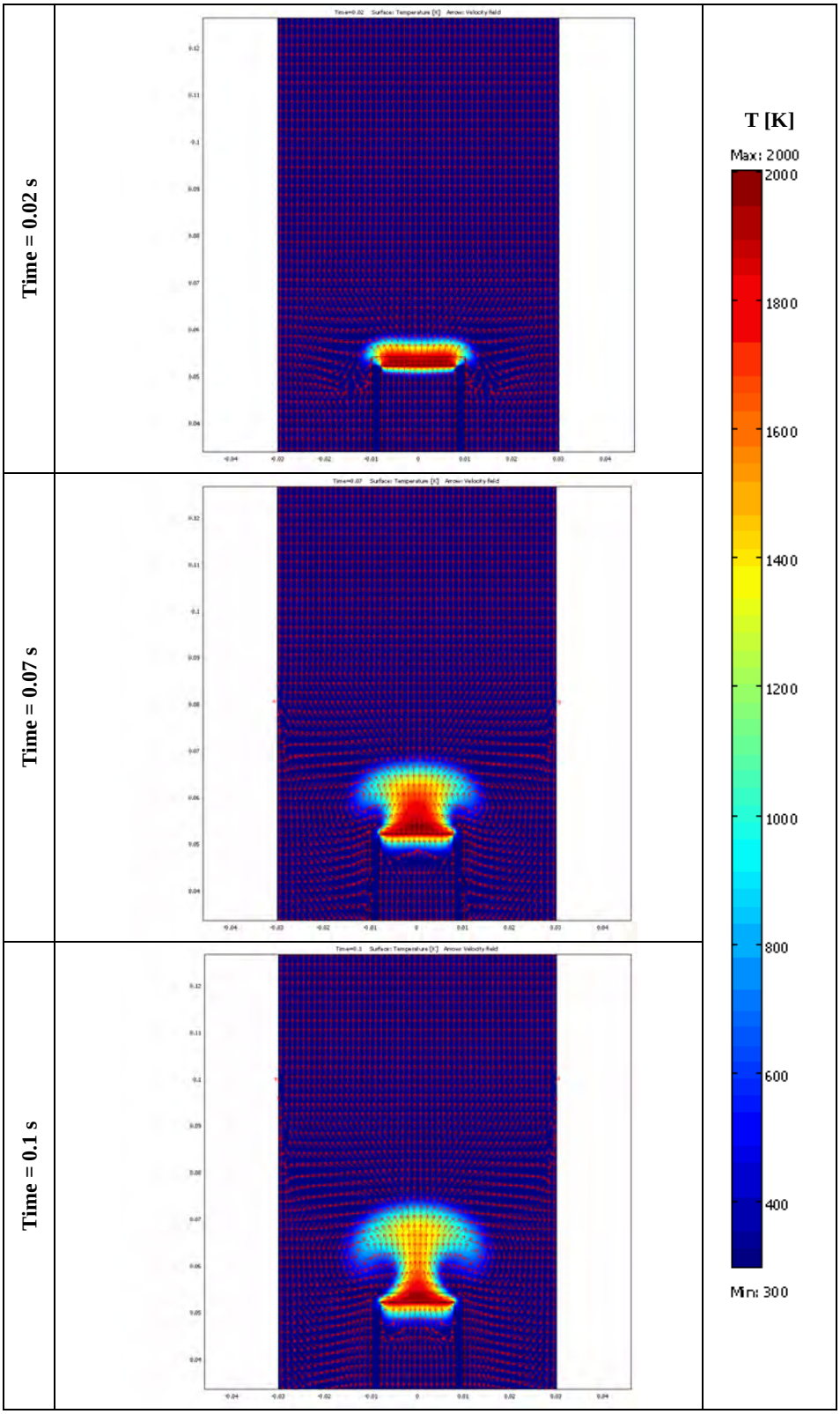

Figure 3. Temperature profile and gas flow along time, considering a distance between the electrodes of 20 mm.

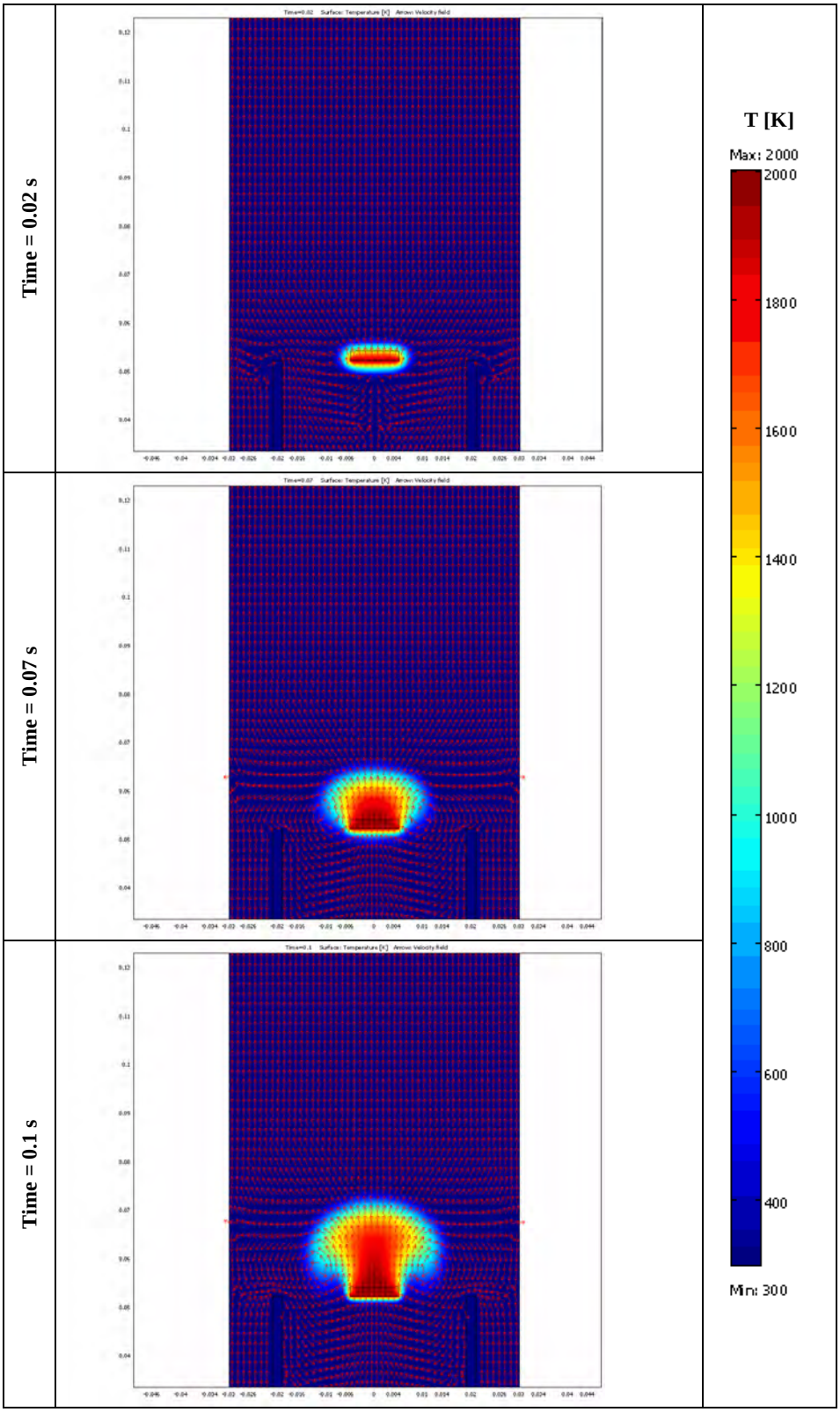

Figure 4. Temperature profile and gas flow along time, considering a distance between the electrodes of 40 mm.

Tables

Table 1. Mesh properties.

Distance between electrodes	Minimum element quality	Degrees of freedom
[mm]	[-]	[-]
10	0.7378	84387
20	0.7730	90373
40	0.8219	58574

Table 2. Governing equations.

	Gas domain (Air)	Electrodes domain (Steel)
Momentum equation	$\rho_{air} c_{P,air} \frac{\partial T}{\partial t} = \mathrm{div}\left(\lambda_{air}\ \mathrm{grad}\ T\right) - \rho_{air} c_{P,air}\ \vec{u} \cdot \mathrm{grad}\ T$	not applicable
Continuity equation	$\frac{\partial \rho_{air}}{\partial t} + \nabla \cdot \left(\rho_{air}\ \vec{u}\right) = 0$	not applicable
Heat transfer equation	$\rho_{air} \frac{\partial \vec{u}}{\partial t} + \rho_{air} \left(\vec{u} \cdot \nabla\right)\vec{u} = -\nabla p + \eta_{air} \nabla^2 \vec{u} + \vec{F}$	$\rho_{steel} c_{P,steel} \frac{\partial T}{\partial t} = \mathrm{div}\left(\lambda_{steel}\ \mathrm{grad}\ T\right)$
Buoyancy force	$F_z = \mathrm{g}\left(\rho_{air,ref} - \rho_{air}\right)$	not applicable
Ideal gas law	$\rho_{air} = p / \left(\mathrm{R}_s\ T\right)$	not applicable

Table 3. Boundary settings in the performed simulations.

	Momentum Equation	Heat Transfer Equation
Glass pipe walls	No slip	Thermal insulation
Electrode-air contact surfaces	No slip	Continuity
Upper boundary	Outlet, ambient pressure	Convective flux
Lower boundary of the electrode domain	Continuity	Spark temperature
Other boundaries	Continuity	Continuity